Received: 19 July 2024 | Revised: 15 October 2024 | Accepted: 19 November 2024

DOI: 10.1002/mrm.30398

Magnetic Resonance in Medicine

TECHNICAL NOTE

# Measurement of pulmonary hematocrit using oscillation of hyperpolarized $^{129}$Xe MR signals in blood

**Xiaoling Liu**[1,2] | **Haidong Li**[1,2] | **Hongchuang Li**[1,2] | **Ming Zhang**[1,2] | **Yu Zheng**[1] | **Xiuchao Zhao**[1,2] | **Lei Shi**[1,2] | **Yeqing Han**[1,2] | **Fumin Guo**[1] | **Xin Zhou**[1,2,3]

[1]Key Laboratory of Magnetic Resonance in Biological Systems, State Key Laboratory of Magnetic Resonance and Atomic and Molecular Physics, National Center for Magnetic Resonance in Wuhan, Wuhan Institute of Physics and Mathematics, Innovation Academy for Precision Measurement Science and Technology, Chinese Academy of Sciences-Wuhan National Laboratory for Optoelectronics, Huazhong University of Science and Technology, Wuhan, China

[2]University of Chinese Academy of Sciences, Beijing, China

[3]School of Biomedical Engineering, Hainan University, Haikou, China

**Correspondence**
Xin Zhou, Key Laboratory of Magnetic Resonance in Biological Systems, State Key Laboratory of Magnetic Resonance and Atomic and Molecular Physics, National Center for Magnetic Resonance in Wuhan, Wuhan Institute of Physics and Mathematics, Innovation Academy for Precision Measurement Science and Technology, Chinese Academy of Sciences-Wuhan National Laboratory for Optoelectronics, Huazhong University of Science and Technology, Wuhan 430071, China.
Email: xinzhou@wipm.ac.cn

**Funding information**
the Strategic Priority Research Program of the Chinese Academy of Sciences, Grant/Award Numbers: XDB0540000, XDC0170000; Youth Innovation Promotion Association, CAS, Grant/Award Numbers: 2020330, 2021330;

## Abstract

**Purpose:** To demonstrate the feasibility of measuring pulmonary hematocrit (Hct) in blood in vivo using oscillation of hyperpolarized $^{129}$Xe MR signals and its potential for disease assessment in animal models.

**Methods:** Hyperpolarized $^{129}$Xe dynamic MR spectroscopy was performed on 10 anemia model rats and 10 control rats. A concise model based on hyperpolarized $^{129}$Xe MR signal oscillations was built for calculating pulmonary Hct. Blood tests and chemical shift saturation recovery were conducted on each rat to obtain Hct. Correlations of Hct obtained from different methods were analyzed using *SPSS* 22.0.

**Results:** Hct measurements were strongly correlated with blood test (Spearman correlation coefficient $r = 0.871$, $p < 0.001$) and chemical shift saturation recovery measurements ($r = 0.956$, $p < 0.001$). Hct was $0.198 \pm 0.054$ for the anemic cohort and $0.457 \pm 0.039$ for the control group ($p < 0.001$).

**Conclusion:** We developed an approach that provided a way to quantify changes in pulmonary Hct using oscillations of hyperpolarized $^{129}$Xe signals. This method shows promise for noninvasive pulmonary Hct assessment and disease evaluation.

**KEYWORDS**
anemia, gas exchange function, hematocrit, hyperpolarized $^{129}$Xe, lung

Xiaoling Liu and Haidong Li contributed equally to this work.

Hubei Provincial Key Technology Foundation of China, Grant/Award Number: 2021ACA013; Key Research Program of Frontier Sciences, CAS, Grant/Award Number: ZDBS-LY-JSC004; National Natural Science Foundation of China, Grant/Award Numbers: 21921004, 82127802, 82202119, 82372150; Hubei Provincial Outstanding Youth Fund, Grant/Award Number: 2023AFA112; Major Program (JD) of Hubei Province, Grant/Award Number: 2023BAA021; National Key Research and Development Program of China, Grant/Award Number: 2022YFC2410000

## 1 | INTRODUCTION

Hematocrit (Hct), defined as the volumetric percentage of red blood cells (RBCs) in blood,[1] is sensitive to various physiological and pathological changes.[2–4] Variations in Hct levels are indicative of blood disorders or other medical conditions that affect blood composition. Clinically, Hct serves as a crucial tool for diagnosing blood disorders, including anemia,[5] characterized by a deficiency of RBCs, and polycythemia, a relatively rare disorder marked by an overabundance of RBCs and an increase in blood viscosity.[6] Moreover, Hct is invaluable for monitoring the progression and treatment response of various diseases, including renal disorders and leukemia.[7,8] It also plays a pivotal role in assessing a patient's blood volume and determining transfusion requirements.[9] Accurate Hct measurements are critically needed for these applications.

Typically, Hct levels are measured using blood tests as the percentage of RBCs in the blood. Although blood tests provide a comprehensive overview of Hct levels throughout the circulatory system, they may not fully capture variations in Hct levels within specific organs or tissues.[10] Notably, differences in Hct levels between vessels of varying diameters complicate the accurate measurement of Hct in deep tissues and microvessels, such as pulmonary vessels.[11,12] In addition, the complex microvasculature of the lung, where air–blood exchange occurs, further hinders accurate pulmonary Hct measurements.

Hyperpolarized (HP) $^{129}$Xe gas MRI has emerged as a promising tool for assessing pulmonary function changes caused by various lung diseases.[13–18] Due to the high lipid solubility and sensitivity to environmental changes, $^{129}$Xe exhibits three distinct resonances in the lung, with distinguishable chemical shifts of 0 ppm in lung airspace, about 198 ppm in tissue and plasma (TP), and about 220 ppm for RBCs.[19] These resonances of TP and RBC are referred to as dissolved-phase xenon. HP $^{129}$Xe MR has been used for the measurements of pulmonary Hct using the chemical shift saturation recovery (CSSR) method.[20–22] However, CSSR is time consuming and tends to yield weak signals at short exchange times.[23,24] Additionally, the complex CSSR gas–blood exchange model and the interdependence of its multiple parameters, particularly Hct and the barrier-to-septum ratio ($\delta/d$), could lead to ambiguous interpretations of the results.[25,26] Previous studies demonstrated oscillations of dissolved $^{129}$Xe signals in the lung caused by cardiac motion using CSSR.[27] These signal oscillations are primarily attributed to fluctuations in blood volume within the pulmonary capillaries during cardiac motion. This finding offers new avenues for measuring pulmonary Hct using HP $^{129}$Xe signal oscillations.

In this study, we presented a theoretical model and an acquisition strategy for pulmonary Hct measurement based on the oscillations of the dissolved $^{129}$Xe signals in the lung. Hct values measured using our method were compared with those obtained from blood tests and CSSR. Additionally, Hct changes due to anemia were also evaluated by the proposed method in an animal model.

## 2 | THEORY

Dissolved-phase $^{129}$Xe signals exhibit high sensitivity to cardiac motion, marked by oscillations that align with the cardiac cyclical activities.[27] These oscillations are postulated to arise from volumetric fluctuations in the pulmonary vascular bed due to cardiac motion.[27–29] Using this phenomenon, a theoretical model for quantifying pulmonary Hct was developed in this study.

Because blood is primarily composed of plasma and RBCs, the remaining elements, such as leukocytes and platelets, constitute less than 1% of the total blood volume.[30] Consequently, Hct can be calculated as follows:

$$\mathrm{Hct} = \frac{V_{\mathrm{RBC}}}{V_{\mathrm{RBC}} + V_{\mathrm{plasma}}} \quad (1)$$

where $V_{\mathrm{RBC}}$ and $V_{\mathrm{plasma}}$ are the volumes of RBCs and plasma in the blood, respectively.

Previous studies show that there is negligible impact of cardiac motion on Hct measurements.[31–33] Therefore, we think that Hct of pulmonary vasculature mirrors Hct of the oscillating blood throughout the cardiac cycle. Consequently, the volumes of RBCs and plasma in Eq. (1) could be replaced with the oscillation volumes of RBCs and plasma over one cardiac cycle, as follows:

$$\mathrm{Hct} = \mathrm{Hct}_{\mathrm{OSC}} = \frac{V_{\mathrm{RBC\_osc}}}{V_{\mathrm{RBC\_osc}} + V_{\mathrm{plasma\_osc}}} \quad (2)$$

where $\mathrm{Hct}_{\mathrm{OSC}}$ denotes Hct derived from oscillating blood during a cardiac cycle, and $V_{\mathrm{RBC\_osc}}$ and $V_{\mathrm{plasma\_osc}}$ represent the oscillating volumes of RBCs and plasma, respectively.

To establish a quantifiable metric in MR experiments, it is essential to correlate the signal intensity of $^{129}$Xe with the volumes of RBCs and plasma. Upon inhalation, xenon gas dissolves into lung tissue, plasma and RBCs, reaching a dynamic equilibrium after a sufficient long exchange time.[20,21] Consequently, the signal intensity of dissolved $^{129}$Xe ($S$) is proportional to the volume ($V$) of the alveolar components, as follows:

$$S = k\lambda V \quad (3)$$

where $k$ represents the factors caused by polarization, acquisition parameters, and hardware performance; and $\lambda$ denotes the solubility of xenon in RBCs, plasma, or lung tissue. As such, the volume oscillations in RBCs and plasma could be rewritten as follows:

$$V_{\mathrm{RBC\_osc}} = \frac{S_{\mathrm{RBC\_osc}}}{k_{\mathrm{RBC}}\lambda_{\mathrm{RBC}}} \quad (4)$$

$$V_{\mathrm{plasma\_osc}} = \frac{S_{\mathrm{plasma\_osc}}}{k_{\mathrm{TP}}\lambda_{\mathrm{plasma}}} \quad (5)$$

where $S_{\mathrm{RBC\_osc}}$ and $S_{\mathrm{plasma\_osc}}$ are the amplitudes of $^{129}$Xe signal oscillations in RBCs and plasma, respectively; $k_{\mathrm{RBC}}$ and $k_{\mathrm{TP}}$ are the scaling factors of $^{129}$Xe signal in RBCs and plasma, respectively; and $\lambda_{\mathrm{RBC}}$ and $\lambda_{\mathrm{plasma}}$ are the Ostwald solubility coefficients of xenon in RBCs (0.27) and plasma (0.09), respectively.[34] Combining Eqs. (1), (4) and (5), Eq. (2) could be rewritten as follows:

$$\begin{aligned}\mathrm{Hct} &= \frac{S_{\mathrm{RBC\_osc}}/\lambda_{\mathrm{RBC}}}{S_{\mathrm{RBC\_osc}}/\lambda_{\mathrm{RBC}} + S_{\mathrm{plasma\_osc}}/\lambda_{\mathrm{plasma}}} \\ &= \frac{1}{1 + \frac{k_{\mathrm{RBC}}}{k_{\mathrm{TP}}} \times \frac{\lambda_{\mathrm{RBC}}}{\lambda_{\mathrm{plasma}}} \times \frac{S_{\mathrm{plasma\_osc}}}{S_{\mathrm{RBC\_osc}}}}\end{aligned} \quad (6)$$

To determine Hct, the ratio $k_{\mathrm{RBC}}/k_{\mathrm{TP}}$ should be calculated. Two approaches can be used: the first involves accurately determining the exact value of proportionality factor, whereas the second simplifies the process by selecting acquisition parameters that minimize the difference between $k_{\mathrm{RBC}}$ and $k_{\mathrm{TP}}$, thereby reducing the influence of $k$. The latter approach is more practical and less complex. Assuming consistent polarization and hardware performance, attention is primarily directed toward acquisition parameters, exchange rates, and relaxation properties. To mitigate the effect of radiofrequency (RF) effects, the RF excitation should be centered between the RBC and TP resonance frequencies, and a pulse with a symmetrical excitation profile should be used. This ensures that both compartments are exposed to uniform RF conditions. Although the RBC and TP compartments may exhibit different exchange rates, choosing a sufficiently long exchange time allows the measured signal to predominantly reflect the compartment volumes rather than the exchange kinetics. For relaxation effects, an apparent $T_1$ fitting can be applied to account for differences in $T_1$ relaxation between compartments. Additionally, during data processing, $T_2^*$ effects can be corrected by incorporating the full width at half maximum in the peak fitting procedure, ensuring accurate signal quantification for both compartments. By following this approach, we can reasonably assume that $k_{\mathrm{RBC}}/k_{\mathrm{TP}} \approx 1$.

Because the $^{129}$Xe signal in the TP compartment originates from both tissue and plasma, and given that the tissue volume remains essentially constant during cardiac motion, we attribute the oscillations observed in the $^{129}$Xe TP signal to variations in plasma volume. Therefore, $S_{\mathrm{plasma\_osc}}$ could be rewritten as follows:

$$S_{\mathrm{plasma\_osc}} = S_{\mathrm{TP\_ocs}} \quad (7)$$

where $S_{\mathrm{TP\_osc}}$ are the amplitudes of $^{129}$Xe signal oscillations in TP. Then, Eq. (6) could be rewritten as follows:

$$\mathrm{Hct} = \frac{1}{1 + \frac{\lambda_{\mathrm{RBC}}}{\lambda_{\mathrm{plasma}}} \times \frac{S_{\mathrm{TP\_ocs}}}{S_{\mathrm{RBC\_osc}}}} \quad (8)$$

Therefore, Hct could be obtained by extracting the ratio of $S_{\mathrm{TP\_osc}}/S_{\mathrm{RBC\_osc}}$ from the dynamic MR sequence. Given the excellent synchronization of the pulsations in both TP and RBC peaks,[27] the signal intensity of RBC and TP can be expressed as follows[28]:

$$S_{\mathrm{RBC}}(t) = S_{\mathrm{RBC\_con}} + S_{\mathrm{RBC\_osc}} \times \sin(2\pi ft + \varphi) \quad (9)$$

$$S_{\mathrm{TP}}(t) = S_{\mathrm{TP\_con}} + S_{\mathrm{TP\_ocs}} \times \sin(2\pi ft + \varphi) \quad (10)$$

where $S_{\mathrm{RBC}}(t)$ and $S_{\mathrm{TP}}(t)$ are the signal intensities of RBC and TP, respectively; $S_{\mathrm{RBC\_con}}$ and $S_{\mathrm{TP\_con}}$ are the constant

$^{129}$Xe signal intensity in RBC and TP, respectively; $f$ is the cardiac frequency; and $\varphi$ is a phase offset.

Before further analysis, $S_{RBC\_con}$ and $S_{TP\_con}$ were obtained using temporal averaging.[28] Subtracting the average values, $S_{RBC\_con}$ and $S_{TP\_con}$, from $S_{RBC}(t)$ and $S_{TP}(t)$, respectively, fast Fourier transform is subsequently applied to both Eqs. (9) and (10), to transform time-domain signals into their corresponding frequency-domain representations. Within the frequency domain, each sinusoidal function generates a peak at its designated frequency. The magnitude of this peak directly corresponds to the amplitude of the time-domain sinusoidal function.[35] The signal intensity at frequency $\omega = f$ was used to ascertain the amplitude ratio $S_{TP\_osc}/S_{RBC\_osc}$. Then, Hct can be calculated using Eq. (8).

## 3 | METHODS

### 3.1 | $^{129}$Xe polarization and delivery

Isotopically enriched xenon gas (86% $^{129}$Xe) was polarized using a commercial polarizer (verImagin Healthcare, Wuhan, China) in a continuous mode. The available polarization of xenon gas in the Tedlar bag was approximately 40%. Polarized xenon gas was administered to the rats using a home-built, MR-compatible gas delivery system, which was controlled by a home-built *LabVIEW* program.[36,37] During MR examinations, the rat was ventilated with xenon and oxygen gas alternately, and the airway pressure of the lung was monitored in real time.

### 3.2 | Animal preparation

All the experiments were conducted with the approval of the institutional review board and in compliance with all relevant ethical guidelines. Twenty male Sprague–Dawley rats (body weight: 180 ± 20 g) were randomly assigned to the experimental ($n = 10$) and control group ($n = 10$). Rats in the experimental group received intraperitoneal injections of phenylhydrazine (40 mg/kg, once a day for 2 days) to generate an anemic rat model.[38,39] Meanwhile, rats from the control group received an intraperitoneal injection of an equivalent volume of saline.

Before MR acquisition, the rats were anesthetized with pentobarbital sodium (30 mg/kg, intraperitoneal injection) and maintained with isoflurane (2%). After tracheotomy, rats were intubated with a catheter (14 gauge) and then connected to the gas delivery system.[37] The rats were alternately ventilated with oxygen or hyperpolarized xenon gas with a tidal volume of 2.5 mL, and the pressure of the trachea was less than 15 cm $H_2O$.

### 3.3 | Data acquisition

Data acquisitions were performed on the second day after the last injection. Before $^{129}$Xe MR measurements, blood samples were collected from the orbit for subsequent blood tests. All MR examinations were performed on a 7T animal MRI scanner (Bruker Biospec 70/20 USR, Germany) using a home-built birdcage coil.[37] CSSR and dynamic MR spectroscopy were performed on each rat.

Schematic of the breathing strategy and $^{129}$Xe MRS pulse sequences are shown in Figure 1. Following the final xenon inhalation, $^{129}$Xe MR data were collected during a controlled breath-hold. For CSSR data collection, two Gaussian-shaped RF pulses centered at the dissolved $^{129}$Xe resonance (approximately 204 ppm) with durations of 0.5 and 0.3 ms were used for saturating and exciting the MR signals of dissolved $^{129}$Xe in the lung, respectively. Spectra were acquired with a bandwidth of 25 kHz and 1024 sampling points, using 24 exchange time points ranging from 2 to 400 ms.[37] For dynamic MR spectroscopy acquisition, a Gaussian-shaped RF pulse, centered at the dissolved $^{129}$Xe resonance with a duration of 0.3 ms was used, and 55 spectra were collected with the following acquisition parameters: repetition time = 50 ms, flip angle = 90°, repetitions = 55, bandwidth = 25 kHz, and sampling points = 1024. The first five spectra were excluded from further analysis. Additionally, only the first 128 sampling points were used for subsequent analysis of the dynamic spectra data, while 512 points were used for CSSR data to improve the signal-to-noise ratio, considering the $T_2$* of both the dissolved phase and gaseous xenon. The $T_2$* of the gaseous xenon is approximately 4 ms, while the corresponding values for TP and RBC are approximately 0.5 ms and 0.7 ms, respectively.

The repetition time of 50 ms was chosen to meet the Nyquist sampling criterion for accurate measurement of cardiac rates.[40] Additionally, within the interval of 50 ms, xenon reaches near dynamic equilibrium in alveolar spaces, RBCs, tissues, and plasma.[37,41] Therefore, the intensity of $^{129}$Xe signal oscillation would accurately reflect actual volume changes rather than exchange rate. Using the peak intensity ratio directly after Fourier transformation aims to minimize error accumulation associated with individually fitting signal oscillation amplitudes, a critical consideration given the high signal oscillation frequency and low oscillation amplitude observed in our rat model.[27]

### 3.4 | Data processing

All MR data sets were processed using *MATLAB* (The MathWorks, Inc., Natick, MA, USA). Signal intensity and chemical shift of RBC and TP were extracted using an

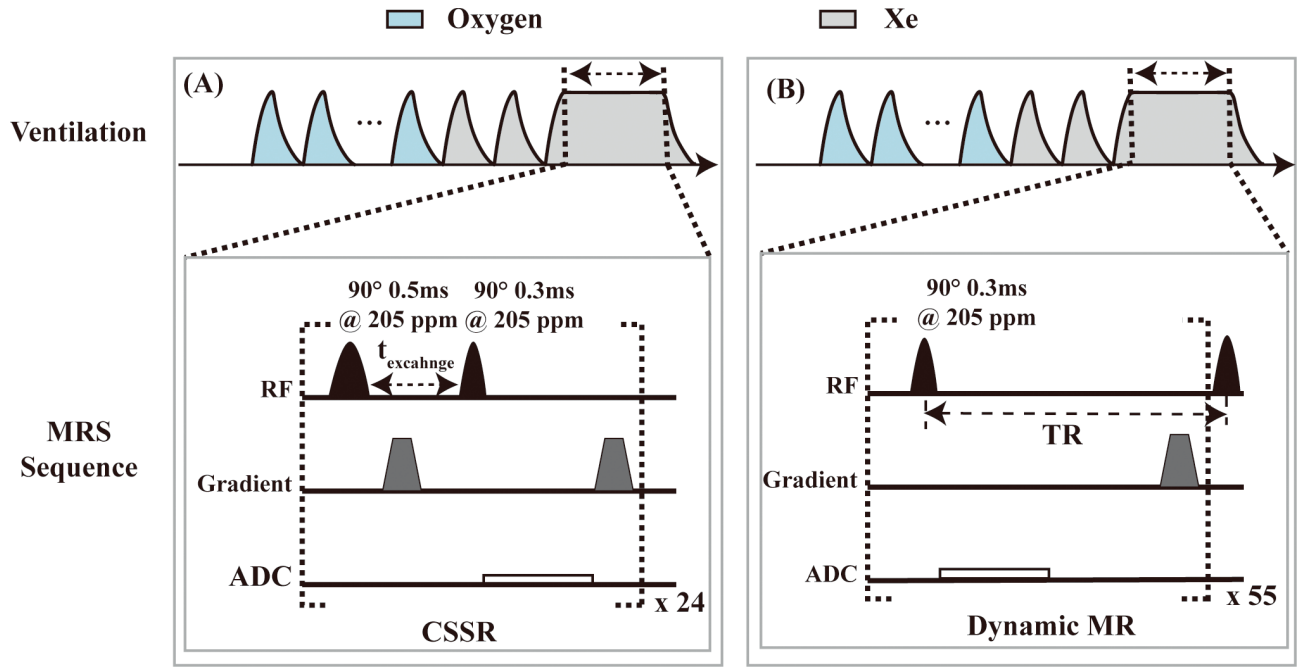


**FIGURE 1** Schematic of the breathing strategy and $^{129}$Xe MRS pulse sequences for chemical shift saturation recovery (CSSR) (A) and dynamic MR spectroscopy (MRS) (B). A respiratory cycle includes multiple oxygen inhalations, followed by three xenon breaths. Following the final xenon inhalation, $^{129}$Xe MR data acquisition was performed during the breath hold. ADC, apparent diffusion coefficient; RF, radiofrequency; TR, repetition time.

open-source toolkit,[42] and the $T_2$* effect was corrected using full width at half maximum in the peak fitting procedure. The Hct was derived from CSSR measurements using the MOXE model.[21,25,37,43]

The dynamic MR spectra were first corrected by fitting $^{129}$Xe signals in TP and RBC to a single exponential decay, $S(t) = A \times e^{-t/T1_{app}}$, to mitigate the effects of apparent $T_1$.[27,28] In this equation, $A$ is the corrected signal intensity; $t$ is the time index of one spectrum in the dynamic series; and $T1_{app}$ is the apparent $T_1$ of signal decay, which includes the effects of $T_1$ relaxation, RF depolarization, and air–blood exchange. The average corrected $^{129}$Xe MR signal intensities in RBC and TP were obtained and subtracted as described in Section 2. Subsequently, the average-removed $^{129}$Xe signal intensities in RBC and TP were transformed to the frequency-domain using fast Fourier transform. The peak signal intensities of RBC and TP, denoted as $S_{RBC\_osc}$ and $S_{TP\_osc}$, were obtained. Hct was obtained using Eq. (8). A typical workflow for $^{129}$Xe dynamic MR spectroscopy data analysis in rats is presented in Figure 2. The SNR of the spectra after fast Fourier transform (corresponding to Figure 2F) are summarized in Table S1.

### 3.5 | Statistical analysis

All the statistical analyses were conducted using *SPSS* 22.0 (IBM Corp., Armonk, NY, USA). An independent t-test was used to compare the measured physiological parameters between the anemia and control groups. Spearman correlation coefficients were used to determine the relationship between Hct provided by various methods. A statistical significance level of $p < 0.05$ was considered.

## 4 | RESULTS

Hct was successfully measured for each rat using all three methods, and these measurements are summarized in Table 1. There were significant differences in Hct between the anemia and control groups measured with blood tests ($0.221 \pm 0.012$ vs. $0.394 \pm 0.055$, $p < 0.001$), CSSR ($0.112 \pm 0.014$ vs. $0.209 \pm 0.011$, $p < 0.001$), and the proposed method ($0.198 \pm 0.0540$ vs. $0.457 \pm 0.039$, $p < 0.001$). These comparisons are illustrated in Figure 3A. Hct obtained using the proposed method was strongly correlated with CSSR ($r = 0.956$, $p < 0.001$) and blood tests ($r = 0.871$, $p < 0.001$), as shown in Figure 3B,C. Bland–Altman plots comparing Hct obtained from different methods are presented in Figure S1.

Significant differences were found in RBC/TP and the chemical shift of TP between the two groups ($p < 0.001$). RBC/TP ratios were $0.174 \pm 0.048$ for the anemia group and $0.385 \pm 0.054$ for the control group ($p < 0.001$). The chemical shift of $^{129}$Xe signal in TP were $196.55 \pm 0.18$ ppm and $196.13 \pm 0.28$ ppm for the anemia and control groups ($p < 0.001$), respectively.

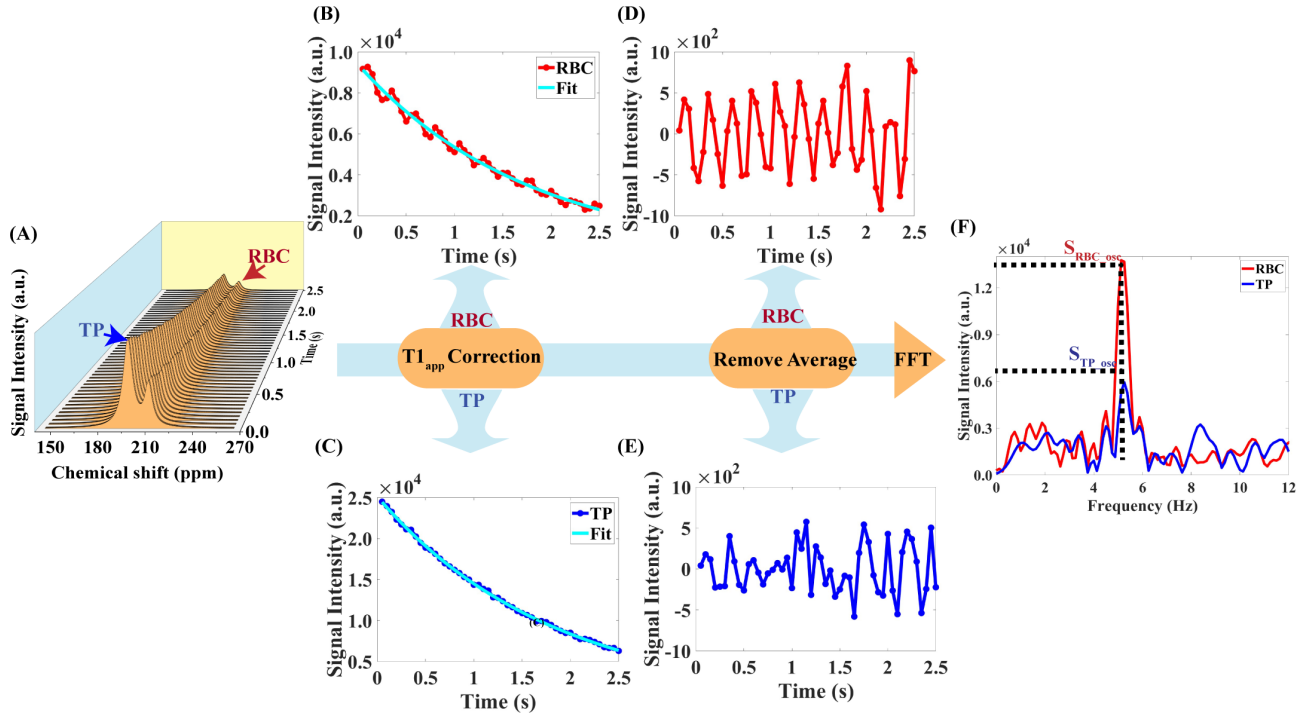


**FIGURE 2** Workflow for $^{129}$Xe dynamic MR spectroscopy data analysis. (A) The dynamics of $^{129}$Xe signal in red blood cells (RBCs) and tissue and plasma (TP) measured from a typical control rat. The corrected $^{129}$Xe signal in RBC (B) and TP (C) with apparent $T_1$. The average-removed $^{129}$Xe signal intensities in RBC (D) and TP (E). (F) Spectra of $^{129}$Xe signal oscillations in RBC and TP after fast Fourier transform (FFT). The $S_{RBC\_osc}$ and $S_{TP\_osc}$ values were used for calculating pulmonary hematocrit.

**TABLE 1** Parameters measured with different methods in anemia and control groups.

| Parameters (Mean ± SD) | Methods | Control ($n = 10$) | Anemia ($n = 10$) | $p$-Value |
|---|---|---|---|---|
| Hct | Blood tests | 0.394 ± 0.055 | 0.221 ± 0.012 | < 0.001*** |
| | CSSR | 0.209 ± 0.011 | 0.112 ± 0.014 | < 0.001*** |
| | Dynamic MR spectroscopy | 0.457 ± 0.039 | 0.198 ± 0.054 | < 0.001*** |
| RBC/TP | Dynamic MR spectroscopy | 0.385 ± 0.054 | 0.174 ± 0.048 | < 0.001*** |
| $\delta_{RBC}$ (ppm) | | 210.42 ± 0.57 | 209.20 ± 1.83 | 0.059 |
| $\delta_{TP}$ (ppm) | | 196.55 ± 0.18 | 196.13 ± 0.28 | < 0.001*** |

Abbreviations: CSSR, chemical shift saturation recovery; Hct, hematocrit; RBC, red blood cells. RBC/TP, the ratio of $^{129}$Xe signal in red blood cells versus barrier (lung tissue and plasma); SD, standard deviation; $\delta_{RBC}$, $^{129}$Xe chemical shift in red blood cells; $\delta_{TP}$, $^{129}$Xe chemical shift in lung tissue and plasma.
***Two-tailed t-test, $p < 0.001$.

## 5 | DISCUSSION

In this study, Hct was measured in vivo using the oscillations of dissolved $^{129}$Xe signal in the lung. Hct obtained using the proposed method was strongly correlated with that derived from blood tests and CSSR. In addition, this method was used to evaluate the changes in Hct induced by anemia in rats. These initial findings demonstrate the potential of using the proposed approach to measure pulmonary Hct with additional capability of assessing changes in Hct caused by various diseases.

The Hct values determined through our proposed method demonstrated strong correlation with blood test measurements and the capability of detecting Hct changes induced by anemia in rats. By capturing Hct levels in blood undergoing volume changes due to cardiac motion, our method provides a way to measure the intrinsic Hct within the pulmonary vasculature. This methodology relies on the assumption that the ratio of oscillating plasma volume ($V_{plasma\_osc}$) to oscillating red blood cell volume ($V_{RBC\_osc}$) is equivalent to the static ratio ($V_{plasma}/V_{RBC}$), indicating negligible Hct variation within the pulmonary vasculature

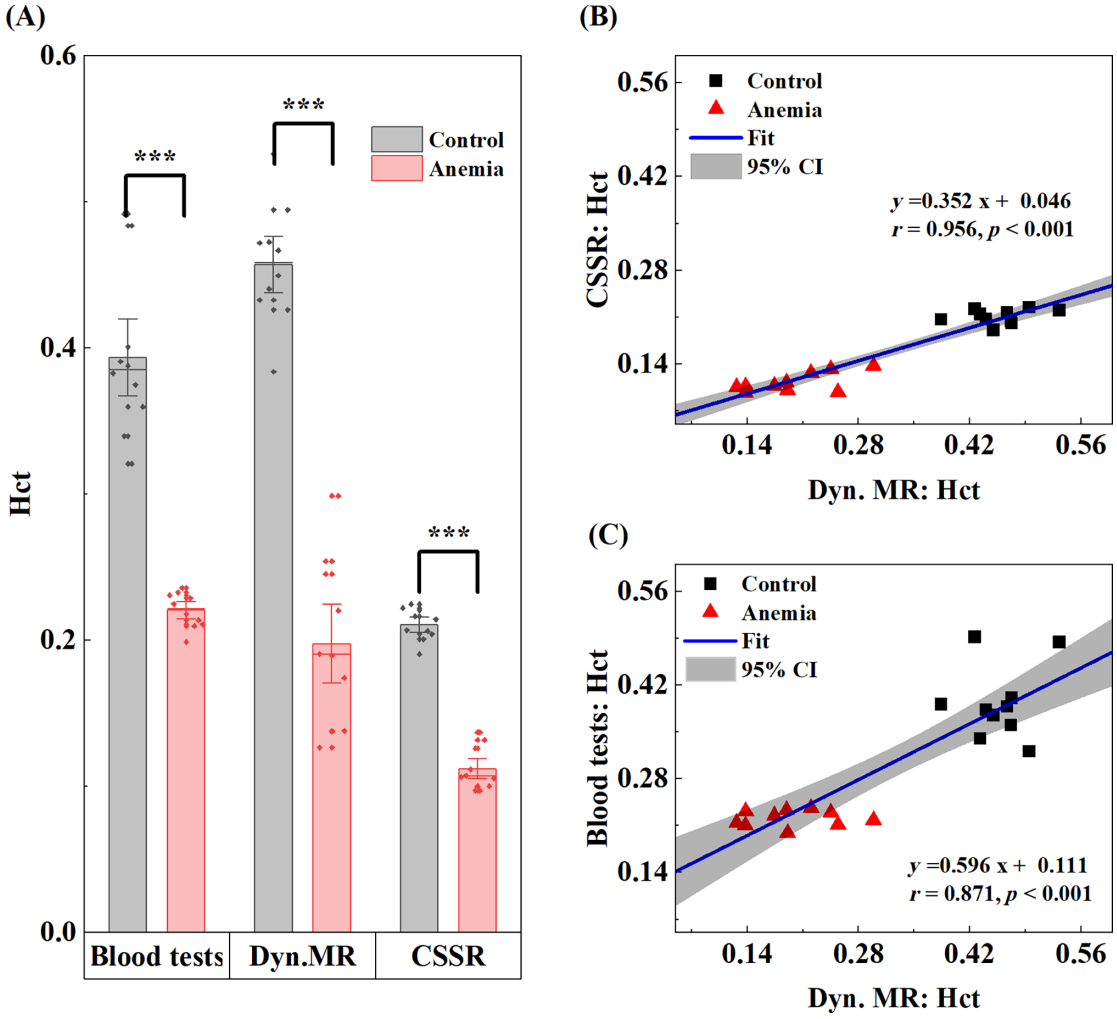


**FIGURE 3** Comparison and correlation analysis of measurement metrics using $^{129}$Xe MR and blood tests. (A) Comparisons of the measured hematocrit (Hct) with different methods between control and anemic rats. Significantly decreased Hct was observed in anemic rats when compared with that in the control group using all three methods. (B) Correlation of the measured Hct with the proposed method and blood tests. (C) Correlation of the Hct measurements with the proposed method and chemical shift saturation recovery (CSSR). CI, confidence interval.

during both systole and diastole.[31] This assumption is grounded in the observation that changes in vascular diameter during cardiac motion are minimal, with signal oscillation amplitudes about 5%. Such small variations are unlikely to produce significant changes in the Hct. Previous studies have also supported this hypothesis through experimental or theoretical simulations.[31–33] Although further validation is necessary, our preliminary findings suggest that this methodology effectively measures changes in pulmonary Hct caused by anemia in agreement with traditional blood test results.

Compared with CSSR, our proposed method yielded substantially higher Hct measurements that were in closer alignment with blood test results. This difference may be attributed to challenges in distinguishing $^{129}$Xe signals originating from plasma versus tissue due to their shared chemical shift. Existing CSSR models, such as MOXE, may mistakenly assign a portion of the tissue signals to the plasma signals.[43] This could result in overestimation of the plasma volume and underestimation of Hct, as evidenced by previous studies in which Hct measured with CSSR was significantly lower than that obtained from blood tests.[25,37,43,44] However, in the proposed method, $^{129}$Xe signals in plasma and tissue were effectively separated by cardiac motion. Specifically, the $^{129}$Xe signal in the plasma would oscillate with the heart motion, while the $^{129}$Xe signal within the tissue remained relatively unaffected.

The anemia rat model induced by phenylhydrazine was used to demonstrate the feasibility of using our proposed method to assess Hct changes induced by anemia. The anemia model replicates pathophysiological changes observed in various types of anemia,[38] primarily oxidative

damage to erythrocytes, accelerating RBC breakdown and reducing Hct levels.[38,45] All three methods revealed significantly lower Hct levels in the anemia group, with the anemic rats exhibiting a significant decrease in RBC/TP ratio, reflecting RBCs' destruction. The significant decline in the TP chemical shift in the anemic rats suggests altered plasma composition due to hemolytic anemia.[39]

As a proof-of-concept study, our research could be expanded in several ways. In this study, dynamic hematocrit during cardiac motion was used to represent the static hematocrit within the pulmonary vasculature. Although the obtained hematocrit results showed a good correlation with CSSR and blood tests, future research should incorporate other methods for validation to serve as a comparative benchmark. Moreover, the feasibility of the proposed method for assessing pulmonary Hct was demonstrated in animal models, and the following studies could verify its feasibility in human. Given the higher signal oscillation amplitudes and lower oscillation frequencies observed in humans, our method shows promise for use in human studies. Meanwhile, global pulmonary Hct was measured with the proposed method, and the local assessment of Hct within the lung could be considered in the further studies.[28,46] For example, with the keyhole techniques,[29,47] which have been used for oscillation amplitude mapping in humans, our method could potentially enable local pulmonary Hct measurement. Additionally, the development of advanced theoretical models is essential for extracting comprehensive physiological parameters, particularly for assessing diseases related to cardiac or pulmonary blood flow abnormalities. For the Hct calculation, we simplified the model by carefully optimizing the acquisition parameters. However, various factors may still affect the accuracy of the results. Future studies could incorporate more sophisticated modeling approaches, such as Bloch simulations, to enhance precision and improve the reliability of these measurements.

## 6 | CONCLUSIONS

In this study, we proposed a new method for assessing pulmonary Hct using the properties of dissolved $^{129}$Xe MR signal oscillations. Hct measured with the proposed method was strongly correlated with that provided by CSSR and traditional blood tests and could be used for assessing the Hct changes caused by anemia in animal, suggesting its potential application for assessment of Hct changes caused by lung diseases.

## ACKNOWLEDGMENTS

This work is supported by National Key Research and Development Program of China (2022YFC2410000), National Natural Science Foundation of China (82127802, 21921004, 82372150, 82202119), the Strategic Priority Research Program of the Chinese Academy of Sciences (XDB0540000, XDC0170000), Key Research Program of Frontier Sciences, CAS (ZDBS-LY-JSC004), Hubei Provincial Key Technology Foundation of China (2021ACA013), Major Program (JD) of Hubei Province (2023BAA021), and Hubei Provincial Outstanding Youth Fund (2023AFA112). Haidong Li and Xiuchao Zhao acknowledge the support from Youth Innovation Promotion Association, CAS (2020330 and 2021330).

## ORCID

*Hongchuang Li* https://orcid.org/0000-0002-7053-9699
*Xin Zhou* https://orcid.org/0000-0002-5580-7907

## REFERENCES

1. Walker HK, Hall WD, Hurst JW, eds. *Clinical Methods: The History, Physical, and Laboratory Examinations*. 3rd ed. Butterworths; 1990.
2. Mairbäurl H. Red blood cell function in hypoxia at altitude and exercise. *Int J Sports Med.* 1994;15:51-63.
3. Etim NN, Williams ME, Akpabio U, Offiong EE. Haematological parameters and factors affecting their values. *Agric Sci.* 2014;2:37-47.
4. Arboix A, Jimenez C, Massons J, Parra O, Besses C. Hematological disorders: a commonly unrecognized cause of acute stroke. *Expert Rev Hematol.* 2016;9:891-901.
5. Christensen RD, Bahr TM, Tweddell SM, Ohls RK, Henry E. Diagnosing anemia in neonates: an evidence-based approach. *NeoReviews.* 2023;24:e343-e355.
6. Tefferi A, Barbui T. Polycythemia vera: 2024 update on diagnosis, risk-stratification, and management. *Am J Hematol.* 2023;98:1465-1487.
7. Talpaz M, Kiladjian JJ. Fedratinib, a newly approved treatment for patients with myeloproliferative neoplasm-associated myelofibrosis. *Leukemia.* 2021;35:1-17.
8. Hingorani S, Gooley T, Pao E, Sandmaier B, McDonald G. Urinary cytokines after HCT: evidence for renal inflammation in the pathogenesis of proteinuria and kidney disease. *Bone Marrow Transplant.* 2014;49:403-409.
9. Carson JL, Stanworth SJ, Dennis JA, et al. Transfusion thresholds for guiding red blood cell transfusion. *Cochrane Database Syst Rev.* 2021;12:CD002042.
10. Calamante F, Ahlgren A, van Osch MJ, Knutsson L. A novel approach to measure local cerebral haematocrit using MRI. *J Cereb Blood Flow Metab.* 2016;36:768-780.
11. Brudin LH, Valind SO, Rhodes CG, Turton DR, Hughes JM. Regional lung hematocrit in humans using positron emission tomography. *J Appl Physiol.* 1986;60:1155-1163.
12. Fåhræus R, Lindqvist T. The viscosity of the blood in narrow capillary tubes. *Am J Physiol.* 1931;96:562-568.
13. Zhou Q, Rao Q, Li H, et al. Evaluation of injuries caused by coronavirus disease 2019 using multi-nuclei magnetic resonance imaging. *Magn Reson Lett.* 2021;1:2-10.
14. Fang Y, Li H, Shen L, et al. Rapid pulmonary $^{129}$Xe ventilation MRI of discharged COVID-19 patients with zigzag sampling. *Magn Reson Med.* 2024;92:956-966.

15. Rao Q, Li H, Zhou Q, et al. Assessment of pulmonary physiological changes caused by aging, cigarette smoking, and COPD with hyperpolarized $^{129}$Xe magnetic resonance. *Eur Radiol.* 2024;34:7450-7459. doi:10.1007/s00330-024-10800-w
16. Zhang M, Li H, Li H, et al. Dynamic evaluation of acute lung injury using hyperpolarized $^{129}$Xe magnetic resonance. *NMR Biomed.* 2024;37:e5078.
17. Zhang M, Li H, Xiao Y, et al. Assessment of global and regional lung compliance in pulmonary fibrosis with hyperpolarized gas MRI. *J Magn Reson Imaging.* 2024. doi:10.1002/jmri.29497
18. Grist JT, Chen M, Collier GJ, et al. Hyperpolarized $^{129}$Xe MRI abnormalities in dyspneic patients 3 months after COVID-19 pneumonia: preliminary results. *Radiology.* 2021; 301:E353-E360.
19. Kern AL, Gutberlet M, Qing K, et al. Regional investigation of lung function and microstructure parameters by localized $^{129}$Xe chemical shift saturation recovery and dissolved-phase imaging: a reproducibility study. *Magn Reson Med.* 2019;81: 13-24.
20. Mansson S, Wolber J, Driehuys B, Wollmer P, Golman K. Characterization of diffusing capacity and perfusion of the rat lung in a lipopolysaccaride disease model using hyperpolarized $^{129}$Xe. *Magn Reson Med.* 2003;50:1170-1179.
21. Chang YV. MOXE: a model of gas exchange for hyperpolarized $^{129}$Xe magnetic resonance of the lung. *Magn Reson Med.* 2013;69:884-890.
22. Zanette B, Santyr G. Accelerated interleaved spiral-IDEAL imaging of hyperpolarized $^{129}$Xe for parametric gas exchange mapping in humans. *Magn Reson Med.* 2019;82:1113-1119.
23. Xie J, Li H, Zhang H, et al. Single breath-hold measurement of pulmonary gas exchange and diffusion in humans with hyperpolarized $^{129}$Xe MR. *NMR Biomed.* 2019;32:e4068.
24. Li H, Zhang Z, Zhao X, et al. Quantitative evaluation of pulmonary gas-exchange function using hyperpolarized $^{129}$Xe CEST MRS and MRI. *NMR Biomed.* 2018;31:e3961.
25. Stewart NJ, Leung G, Norquay G, et al. Experimental validation of the hyperpolarized $^{129}$Xe chemical shift saturation recovery technique in healthy volunteers and subjects with interstitial lung disease. *Magn Reson Med.* 2015;74:196-207.
26. Bechtel A, Lu J, Mummy D, et al. Establishing a hemoglobin adjustment for $^{129}$Xe gas exchange MRI and MRS. *Magn Reson Med.* 2023;90:1555-1568.
27. Ruppert K, Altes TA, Mata JF, Ruset IC, Hersman FW, Mugler JP 3rd. Detecting pulmonary capillary blood pulsations using hyperpolarized xenon-129 chemical shift saturation recovery (CSSR) MR spectroscopy. *Magn Reson Med.* 2016;75:1771-1780.
28. Bier EA, Robertson SH, Schrank GM, et al. A protocol for quantifying cardiogenic oscillations in dynamic $^{129}$Xe gas exchange spectroscopy: the effects of idiopathic pulmonary fibrosis. *NMR Biomed.* 2019;32:e4029.
29. Niedbalski PJ, Bier EA, Wang Z, Willmering MM, Driehuys B, Cleveland ZI. Mapping cardiopulmonary dynamics within the microvasculature of the lungs using dissolved $^{129}$Xe MRI. *J Appl Physiol (1985).* 2020;129:218-229.
30. Mathew J, Sankar P, Varacallo M. *Physiology, Blood Plasma*. StatPearls Publishing; 2023.
31. Silverman DA, Rakusan K. Red blood cell spacing in rat coronary capillaries during the cardiac cycle. *Microvasc Res.* 1996;52:143-156.
32. Chaiken J, Deng B, Goodisman J, Shaheen G, Bussjager RJ. Analyzing near-infrared scattering from human skin to monitor changes in hematocrit. *J Biomed Opt.* 2011;16:97005.
33. Fuchs A, Berg N, Fuchs L, Prahl WL. Assessment of rheological models applied to blood flow in human thoracic aorta. *Bioengineering (Basel).* 2023;10:1240.
34. Chen RY, Fan FC, Kim S, Jan KM, Usami S, Chien S. Tissue-blood partition coefficient for xenon: temperature and hematocrit dependence. *J Appl Physiol Respir Environ Exerc Physiol.* 1980;49:178-183.
35. Keeler J. *Understanding NMR Spectroscopy*. 2nd ed. John Wiley & Sons; 2010.
36. Nouls J, Fanarjian M, Hedlund L, Driehuys B. A constant-volume ventilator and gas recapture system for hyperpolarized gas MRI of mouse and rat lungs. *Concepts Magn Reson Part B Magn Reson Eng.* 2011;39B:78-88.
37. Zhang M, Li H, Li H, et al. Quantitative evaluation of lung injury caused by $PM_{2.5}$ using hyperpolarized gas magnetic resonance. *Magn Reson Med.* 2020;84:569-578.
38. Diallo A, Gbeassor M, Vovor A, et al. Effect of Tectona grandis on phenylhydrazine-induced anaemia in rats. *Fitoterapia.* 2008;79:332-336.
39. Sato H, Sakairi T, Fujimura H, et al. Hematological and morphological investigation of thrombogenic mechanisms in the lungs of phenylhydrazine-treated rats. *Exp Toxicol Pathol.* 2013;65:457-462.
40. Azar T, Sharp J, Lawson D. Heart rates of male and female Sprague-Dawley and spontaneously hypertensive rats housed singly or in groups. *J Am Assoc Lab Anim Sci.* 2011;50:175-184.
41. Fliss JD, Zanette B, Friedlander Y, et al. Hyperpolarized $^{129}$Xe magnetic resonance spectroscopy in a rat model of bronchopulmonary dysplasia. *Am J Physiol Lung Cell Mol Physiol.* 2021;321:L507-L517.
42. Robertson SH, Virgincar RS, Bier EA, et al. Uncovering a third dissolved-phase $^{129}$Xe resonance in the human lung: quantifying spectroscopic features in healthy subjects and patients with idiopathic pulmonary fibrosis. *Magn Reson Med.* 2016;78:1306-1315.
43. Li H, Zhang Z, Zhao X, Sun X, Ye C, Zhou X. Quantitative evaluation of radiation-induced lung injury with hyperpolarized xenon magnetic resonance. *Magn Reson Med*. 2016;76:408-416.
44. Chang YV, Quirk JD, Ruset IC, Atkinson JJ, Hersman FW, Woods JC. Quantification of human lung structure and physiology using hyperpolarized $^{129}$Xe. *Magn Reson Med.* 2014;71:339-344.
45. Djurkovic A, Zaric J, Lusic M, Glisin V, Popovic Z. Differences in rat rbc cytosol induced after in vivo phenylhydrazine treatment. *Cell Biol Int.* 1999;23:677-683.
46. Bier E, Alenezi F, Lu J, Mammarappallil J, Driehuys B, Rajagopal S. Hyperpolarized Xe-129 magnetic resonance oscillation imaging in pulmonary hypertension. *Am J Respir Crit Care Med.* 2021;203:2.
47. Lu J, Alenezi F, Bier E, et al. Optimized quantitative mapping of cardiopulmonary oscillations using hyperpolarized $^{129}$Xe gas exchange MRI: digital phantoms and clinical evaluation in CTEPH. *Magn Reson Med.* 2024;91:1541-1555.

## SUPPORTING INFORMATION

Additional supporting information may be found in the online version of the article at the publisher's website.

**Figure S1.** Bland–Altman plots comparing hematocrit (Hct) values obtained from different methods. (A) Comparison between Hct values from the proposed method and blood tests. (B) Comparison between Hct values from the proposed method and chemical shift saturation recovery (CSSR). (C) Comparison between Hct values from blood tests and CSSR.

**Table S1.** Signal-to-noise ratio (SNR) of the spectrum after fast Fourier transform.

**How to cite this article:** Liu X, Li H, Li H, et al. Measurement of pulmonary hematocrit using oscillation of hyperpolarized $^{129}$Xe MR signals in blood. *Magn Reson Med*. 2024;1-10. doi: 10.1002/mrm.30398